

# Geophysical Research Letters®

## RESEARCH LETTER

10.1029/2022GL097913

### Key Points:

- Intermittent saltation on Titan can be sustained at lower wind speeds than previously thought
- The grains forming Titan dunes may be primarily in the size range 0.05–0.1 mm
- Yearly sediment transport rates on Titan are of the order of  $10^4$  kg m<sup>-1</sup> per Titan year

### Supporting Information:

Supporting Information may be found in the online version of this article.

### Correspondence to:

F. Comola,  
[francesco.comola@gmail.com](mailto:francesco.comola@gmail.com)

### Citation:

Comola, F., Kok, J. F., Lora, J. M., Cohanin, K., Yu, X., He, C., et al. (2022). Titan's prevailing circulation might drive highly intermittent, yet significant sediment transport. *Geophysical Research Letters*, 49, e2022GL097913. <https://doi.org/10.1029/2022GL097913>

Received 20 JAN 2022  
Accepted 17 MAR 2022

## Titan's Prevailing Circulation Might Drive Highly Intermittent, Yet Significant Sediment Transport

F. Comola<sup>1</sup> , J. F. Kok<sup>1</sup> , J. M. Lora<sup>2</sup> , K. Cohanin<sup>1</sup>, X. Yu<sup>3</sup> , C. He<sup>4</sup> , P. McGuiggan<sup>5</sup> , S. M. Hörst<sup>4</sup> , and F. Turney<sup>1</sup>

<sup>1</sup>Department of Atmospheric and Oceanic Sciences, University of California, Los Angeles, CA, USA, <sup>2</sup>Department of Earth and Planetary Sciences, Yale University, New Haven, CT, USA, <sup>3</sup>Department of Earth and Planetary Sciences, University of California, Santa Cruz, CA, USA, <sup>4</sup>Department of Earth and Planetary Sciences, Johns Hopkins University, Baltimore, MD, USA, <sup>5</sup>Department of Materials Science and Engineering, Johns Hopkins University, Baltimore, MD, USA

**Abstract** Titan, the largest moon of Saturn, is characterized by gigantic linear dunes and an active dust cycle. Much like on Earth, these aeolian processes are caused by the wind-driven saltation of surface grains. It is still unclear, however, how saltation on Titan can occur despite the typically weak surface winds and the potentially cohesive surface grains. Here, we explore the hypothesis that saltation on Titan may be sustained at lower wind speeds than previously thought, primarily through granular splash rather than aerodynamic lifting of surface grains. We propose a saltation mass flux parameterization for Titan and use it to quantify sediment transport with a general circulation model. The results suggest that Titan's prevailing circulation can generate highly intermittent yet significant saltation, with mass fluxes of the order of  $10^4$  kg m<sup>-1</sup> year<sup>-1</sup>, and that Titan dunes may be formed primarily by fine grains, approximately 0.1 mm in size.

**Plain Language Summary** The Cassini-Huygens mission has revealed that Titan's landscape evolution and dust cycle may be controlled by the wind-driven transport of surface grains, known as saltation. It is still unclear, however, how saltation can occur on Titan despite the weak winds and the potential stickiness of the surface grains. Using a combination of experiments, theory, and modeling, we find that, like saltation on Mars, saltation on Titan can be sustained at much lower wind speeds than those required to lift grains from the surface. Accordingly, the prevailing weak winds on Titan may be capable of driving intermittent yet significant sediment transport.

## 1. Introduction

The Cassini-Huygens mission revealed that Titan's low-latitude surface presents a variety of landforms (Lopes et al., 2019; Lorenz et al., 2006; MacKenzie et al., 2021), including gigantic linear dunes similar in shape to those of the Namib desert (Lorenz and Zimbleman, 2014; Radebaugh et al., 2008, 2010). Analyses of Cassini spectral data, combined with atmospheric and radiative transfer modeling, have further revealed that Titan presents an active dust cycle (Charnay et al., 2015; Rodriguez et al., 2018). This observational evidence suggests that, much like on Earth, Titan dunes actively evolve by an aeolian, or wind-driven, transport process known as saltation: after being lifted and accelerated by the wind, surface grains hop along the granular bed, rebounding, and splashing other grains into the airflow (Kok et al., 2012; Pähtz et al., 2020).

Titan's sand grains are not made of silicates as on Earth but mainly of solid organics precipitated from the atmosphere (McCord et al., 2006; Soderblom et al., 2007). Even though their physical properties are not precisely known, previous studies have suggested that these organic grains are less dense than quartz sand (He et al., 2017; Hörst & Tolbert, 2013; Imanaka et al., 2012), and potentially more cohesive (Méndez-Harper et al., 2017; Yu, Hörst, He, & McGuiggan, 2020; Yu, Hörst, He, McGuiggan, Kristiansen, Zhang, 2020; Yu et al., 2017). Because Titan's atmosphere is denser than Earth's, it has been commonly assumed that saltation on Titan is similar to sediment transport in water, where surface grains are primarily lifted by fluid forces (Kok et al., 2012). Previous studies have suggested that the typically weak surface winds of Titan's prevailing circulation are hardly strong enough to lift grains from the surface, and that saltation is primarily driven by sporadic equatorial methane storms at equinox (Charnay et al., 2015). However, recent studies have suggested that saltation of cohesive grains, such as those on Titan, can be sustained through rebound and granular splash at much lower wind speeds than those required to trigger aerodynamic lifting of surface grains (Comola, Gaume, et al., 2019; Lorenz et al., 2006; Pähtz

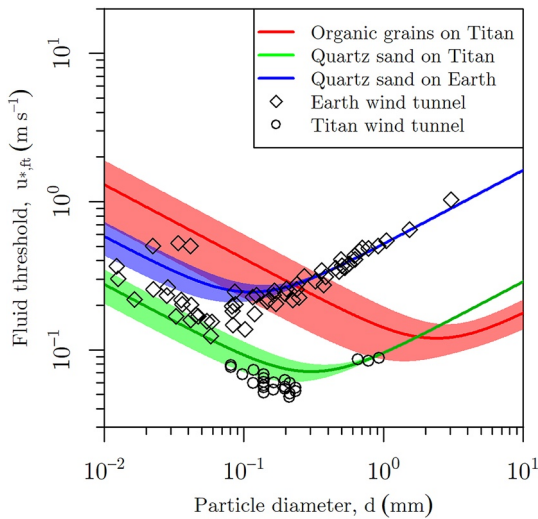


**Figure 1.** Variation in the fluid threshold with particle size on Earth and Titan. The red curve refers to organic grains on Titan, the blue one refers to quartz grains on Earth, and the green one is the hypothetical fluid threshold of quartz grains on Titan. The shaded areas indicate standard errors, obtained by propagating the uncertainties in the cohesion coefficient  $\gamma$  and particle density  $\rho_p$ . Black diamond markers indicate wind tunnel measurements of the fluid threshold in Earth conditions (Bagnold, 1937; Chepil, 1945; Fletcher, 1976; Iversen et al., 1976; Zingg, 1953). Black circles indicate fluid threshold measurements carried out in the Titan wind tunnel (Burr et al., 2015) for sediments with weaker cohesive bonds than organic grains on Titan (silica sand, basaltic sand, glass spheres, and walnut shells).

et al., 2021). The role of Titan's prevailing atmospheric circulation in driving the active dust cycle and landscape evolution may therefore be more relevant than previously thought.

Here, we aim to shed light onto aeolian transport processes on Titan through a combination of laboratory experiments, theory, and numerical modeling. For this purpose, we propose novel parameterizations to quantify the wind speeds required to trigger aerodynamic entrainment and to sustain saltation through granular splash of cohesive grains on Titan. We specify the key physical parameters of these parameterizations, namely grain density, elasticity, and cohesion, based on recent experimental investigations (Yu et al., 2017) and test their performance against the results of a discrete element model. We then account for the proposed entrainment parameterizations in the saltation model comprehensive numerical model of steady state saltation (COMSALT) (Kok & Renno, 2009) to investigate how sediment mass flux scales with friction velocity on Titan. We finally include the mass flux parameterization in the general circulation model Titan Atmospheric Model (TAM) (Faulk et al., 2020; Lora et al., 2015) to quantify yearly sediment transport rates on Titan. We find that Titan's prevailing circulation drives highly intermittent saltation, with transport rates of the order of  $10^4 \text{ kg m}^{-1} \text{ year}^{-1}$ .

## 2. Fluid Threshold on Titan

A correct estimation of the minimum wind speed required to generate aerodynamic lifting of surface grains, the so-called fluid threshold, is essential to understand the conditions that allow for initiation of saltation on Titan. To estimate the fluid threshold, we use the well-known parameterization (Shao & Lu, 2000)

$$u_{*,ft} = \sqrt{A_N \left( \frac{\rho_p}{\rho_f} g d + \frac{\gamma}{\rho_f d} \right)}, \quad (1)$$

where  $A_N = 0.0123$  is an empirical dimensionless parameter,  $g \approx 1.35 \text{ m s}^{-2}$  is the gravitational constant,  $d$  is the particle diameter,  $\rho_f \approx 5.2 \text{ kg m}^{-3}$  is the air density,  $\rho_p \approx 950 \pm 450 \text{ kg m}^{-3}$  is the particle density (uncertainty estimations throughout the paper refer to standard errors), and  $\gamma$  is a cohesion coefficient. Cohesion is related to the intrinsic stickiness of the material (the surface energy), the particle shape and roughness, the stiffness of the contacting grains, and the moisture conditions (Israelachvili, 1986). It is usually assumed that  $\gamma \propto \beta = F_\phi/d$ , that is, the ratio between the cohesive force  $F_\phi$  and the particle size  $d$ . It is important to note that  $\beta$  represents the average cohesive force between grains, whereas  $\gamma$  represents the cohesive force acting on the grains that are more readily lifted by the wind. Because of this discrepancy, the proportionality constant between  $\gamma$  and  $\beta$  is generally unknown. We therefore estimate  $\gamma$  for Titan grains by assuming that the ratio of  $\gamma$  and  $\beta$  is equal on Earth and Titan, that is,

$$\frac{\gamma_T}{\beta_T} = \frac{\gamma_E}{\beta_E}. \quad (2)$$

Measurements of fluid threshold for quartz sand suggest that  $\gamma_E \approx 0.33 \pm 0.17 \text{ mN m}^{-1}$  (Shao & Lu, 2000). Furthermore, laboratory measurements of the cohesive forces for quartz sand and Titan-analog grains, known as tholins, suggest that  $\beta_E \approx 1.2 \text{ mN m}^{-1}$  (Corn, 1961) and  $\beta_T \approx 27 \pm 20 \text{ mN m}^{-1}$  Yu et al. (2017) measured a cohesive force  $F_\phi = 0.8 \pm 0.6 \mu\text{N}$  for tholin particles of size  $d = 30 \mu\text{m}$ . Based on Equation 2 and accounting for error propagation, we estimate that  $\gamma_T \approx 7.3 \pm 6.7 \text{ mN m}^{-1}$ . We use this range of  $\gamma_T$  in Equation 1 to estimate the variation in fluid threshold with particle size (Figure 1). The results indicate that the minimum shear velocity required to lift a grain on Titan (red curve in Figure 1) is  $u_{*,ft} \approx 0.12 \text{ m s}^{-1}$ , which is approximately three times larger than expected if cohesive forces among organic grains on Titan were equal to those among sand particles on Earth (green curve in Figure 1). Furthermore, this minimum value corresponds to a particle size  $d \approx 2 \text{ mm}$ ,

meaning that the particles that are easiest to lift on Titan are roughly one order of magnitude larger than sand particles that are easiest to lift on Earth (blue curve in Figure 1). Critically, we find that previous measurements carried out in a wind tunnel with environmental conditions similar to those on Titan (black circles in Figure 1) may have significantly underestimated the fluid threshold and the size of the more mobile grains on Titan due to the low cohesion of the sediments used for the experiments (Burr et al., 2015; Yu et al., 2017).

### 3. Impact Threshold on Titan

Our analyses have so far suggested that the fluid threshold on Titan may be significantly higher than previously thought due to the high cohesion of surface grains. However, saltation may be sustained through the granular splash process at a potentially lower wind speed, known as the impact threshold  $u_{*,it}$  (Pächt & Durán, 2018). Granular splash is a complex and highly stochastic process controlled by interparticle collisions and cohesive bonds among neighboring grains. To quantify the impact threshold on Titan, we first need to quantify the effect of cohesion on the mean velocity and number of splashed grains. To predict the mean velocity of the splashed grains  $\langle v_s \rangle$ , we extend an expression for loose granular materials (Kok & Renno, 2009) with an additional term that accounts for the potential cohesion among grains on Titan (see Section S1 in Supporting Information S1 for the analytical derivation)

$$\frac{\langle v_s \rangle}{\sqrt{gd}} = \frac{\mu}{a} \left[ 1 - \exp\left(-a \frac{v_i}{\sqrt{gd}}\right) \right] + b \sqrt{\frac{2(1-\delta)\phi}{mgd}}. \quad (3)$$

In Equation 3,  $\phi$  is the elastic energy released upon the breaking of cohesive bonds, and  $\delta \approx 0.3$  is the fraction of elastic energy dissipated. The elastic energy  $\phi$  is a function of the cohesive force  $F_\phi$  and the effective bond elastic modulus  $E$ , which we estimate from experiments on tholin particles (Yu et al., 2017) (see Section S1 and Table S2 in Supporting Information S1). Further,  $\mu \approx 0.15$  is the average fraction of impacting momentum spent on splashing surface particles (Kok & Renno, 2009). The proportionality coefficients  $a \approx 0.03$  and  $b \approx 1.2$ , which scale the contributions of collisional and cohesive forces to the ejection velocity, are assigned based on literature values (Kok & Renno, 2009) and by fitting data from discrete element simulations of splash process over cohesive surfaces (see section S1 in Supporting Information S1).

To estimate the mean number of splashed grains  $\langle N_s \rangle$ , we adopt a splash model derived from the energy and momentum conservation equations (Comola & Lehning, 2017). This model was shown to be in good agreement with a variety of experimental results, including granular splash data of cohesive snow and ice grains. For a granular bed of uniform spherical grains, the average number of splashed grains predicted by the energy conservation equation equals

$$\langle N_e \rangle = \frac{(1 - P_r \epsilon_r - \epsilon_f) u_i^2}{2 \langle v_s \rangle^2 + \frac{12\delta\phi}{\pi \rho_p d^3}}, \quad (4)$$

where  $\epsilon_r$  is the fraction of impact energy retained by the rebounding grain,  $P_r$  is the probability of rebound (Andreotti, 2004; Anderson & Haff, 1991), and  $\epsilon_f$  is the fraction of energy dissipated to the bed. Furthermore, the average number of splashed grains predicted by the horizontal momentum conservation equation equals

$$\langle N_m \rangle = \frac{(1 - P_r \mu_r - \mu_f) v_i \cos \alpha_i}{\langle v_s \rangle \langle \cos \alpha_s \rangle \langle \cos \beta_s \rangle}. \quad (5)$$

where  $\mu_r$  is the fraction of momentum retained by the rebounding grain,  $\mu_f$  is the fraction of momentum lost to the bed,  $\alpha_i$  is the vertical impact angle,  $\cos \alpha_s$  is the cosine of the vertical splash angle, and  $\cos \beta_s$  the cosine of the horizontal splash angle. The values of all parameters in Equations 4 and 5 are assigned based on experimental measurements (Ammi et al., 2009; Nalpanis et al., 1993; Rice et al., 1995, 1996; Willetts & Rice, 1986, 1989) (see Table S1 in Supporting Information S1). Following previous approaches (Comola & Lehning, 2017; Kok & Renno, 2009), we take the number of splashed grains as  $\langle N_s \rangle = \min(\langle N_e \rangle, \langle N_m \rangle)$ , to represent the transition from a momentum-limited to an energy-limited splash process. We discuss the generalizations of Equations 3–5 for mixed-sized granular beds in Section S1 of Supporting Information S1.

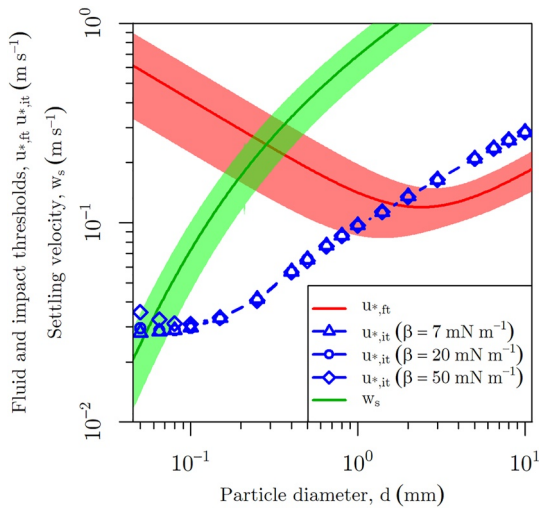


**Figure 2.** Variation in fluid threshold, impact threshold, and settling velocity of grains on Titan. The fluid threshold  $u_{*ft}$  (red curve, also shown in Figure 1) is estimated with Equation 1. The impact threshold  $u_{*it}$  is estimated with the saltation model comprehensive numerical model of steady state saltation for three different values of the cohesion coefficient  $\beta$  (blue curves), which span the whole uncertainty range of cohesive forces among organic grains on Titan. The settling velocity  $w_s$  (green curve) is calculated by balancing the gravitational, drag, and buoyancy forces acting on spherical grains in still air. The shaded areas indicate one standard error from the mean.

We test the predictions of Equations 3–5 against the results of a discrete element model that was previously used to investigate the role of cohesion in the granular splash process (Comola, Gaume, et al., 2019) (see Sections S2 and S3 in Supporting Information S1). Both our splash model and the discrete element simulations suggest that cohesive forces among tholins are barely sufficient to affect the granular splash of particles of size  $d = 0.25$  mm (Figure S4 in Supporting Information S1), and are even less relevant for coarser tholins of size  $d = 2.5$  mm, which are splashed similarly to loose sand grains on Earth.

The small influence of cohesion on the splash process of tholins larger than 0.25 mm suggests that the impact threshold  $u_{*it}$  on Titan may also be weakly affected by cohesion. To investigate this, we implement Equations 3–5 in the comprehensive saltation model COMSALT (Kok, 2010a, 2010b; Kok & Renno, 2009) and simulate Titan saltation for a wide range of cohesive forces (see Sections S4 and S5 in Supporting Information S1 for the implementation details). Critically, we find that cohesive forces do not significantly affect the impact threshold of grains larger than 0.1 mm (blue lines in Figure 2), and only moderately increase the impact threshold of smaller grains. Most importantly, the minimum impact threshold  $u_{*it} \approx 0.03$  m s<sup>-1</sup> is a factor of four smaller than the minimum fluid threshold, suggesting that Titan saltation may be sustained at wind speeds much smaller than those required to initiate it. Furthermore, the minimum impact threshold corresponds to a particle size  $d \approx 0.1$  mm, which is one order of magnitude smaller than the size of particles most easily lifted by aerodynamic forces.

#### 4. Size of Saltating Grains on Titan

Our results have thus far indicated that the minimum fluid threshold corresponds to a particle size  $d \approx 2$  mm, whereas the minimum impact threshold corresponds to a particle size  $d \approx 0.1$  mm. It follows that the size of grains in saltation may depend on the wind speed, that is, saltating grains are coarser near the transport initiation threshold and finer near to the transport cessation threshold.

To investigate the size range of saltating grains, we assume that Titan's surface presents mixed-sized grains in the range 0.05–2 mm, similar to sand grains on Earth. We further assume that, whenever the wind speed exceeds the minimum fluid threshold, all surface grain sizes are susceptible to motion according to the equal susceptibility principle (Martin & Kok, 2019). We follow a similar approach to previous studies (Greeley & Iversen, 1985; Nishimura & Hunt, 2000; Sullivan & Kok, 2017) and investigate the size distribution of grains in saltation by evaluating the ratio  $w_s/u_*$ , where  $w_s$  is the terminal fall velocity as a function of the grain size (green curve in Figure 2). Values of  $w_s/u_*$  near unity indicate that gravitational and turbulent forces are of the same order of magnitude and grain transport is therefore transitional between saltation and suspension. We find that, near the threshold for transport initiation ( $u_* \approx u_{*ft}$ ),  $w_s/u_* > 1$  for  $d > 0.2$  mm, whereas, near the threshold for transport cessation ( $u_* \approx u_{*it}$ ), the ratio  $w_s/u_* > 1$  for  $d > 0.05$  mm. These results suggest that the size of saltating grains at the onset of transport lies in the range  $d \approx 0.2 - 2$  mm, as smaller grains become suspended in turbulent eddies. Conversely, close to the cessation of transport, the size of saltating grains lies in the lower range  $d \approx 0.05 - 0.1$  mm, because the wind speed is not sufficient to sustain saltation of larger grains through rebound and splash.

#### 5. Mass Flux Scaling on Titan

Our analyses indicate that initiation and cessation of saltation on Titan occur at very different wind speeds, yielding a ratio between the impact and fluid thresholds  $u_{*it}/u_{*ft} \approx 0.25$  much smaller than previously thought (Kok et al., 2012). This suggests that saltation on Titan can be sustained at much lower wind speeds than those required to initiate it, similar to the transport mechanisms on Mars (Sullivan & Kok, 2017). We find that the surface wind

speeds in Titan's equatorial band (30°S–30°N) predicted by general circulation models (Lebonnois et al., 2012; Lora et al., 2015; Newman et al., 2016; Tokano, 2010) exceed the impact threshold 15%–30% of Titan's year and can therefore sustain sediment transport (see Section S6 in Supporting Information S1). To quantify the sediment transport rates driven by the prevailing circulation, we derive a saltation mass flux parameterization for Titan conditions and test its accuracy against COMSALT simulations.

Previous studies have suggested that the general expression for the steady-state saltation mass flux reads  $Q = \rho_f (u_*^2 - u_{*,it}^2) L / \langle \Delta v \rangle$ , where  $L$  is the mean hop length of saltating grains and  $\langle \Delta v \rangle$  is the mean difference in grain horizontal velocity before and after impacting the bed (Durán et al., 2011; Kok et al., 2012). In steady-state saltation, the impact velocity is bound to yield a mean replacement capacity equal to 1, that is, to generate on average one splashed grain for every impactor that fails to rebound (Ungar & Haff, 1987). It follows that  $\langle \Delta v \rangle$  is independent of  $u_*$  and rather scales as  $\langle \Delta v \rangle \sim u_{*,it}$ . Conversely, the hop length  $L$  is determined in part by particle speeds higher up in the saltation layer. For saltation on Earth,  $L$  is only a weak function of  $u_*$  and is often assumed to scale as  $L \sim u_{*,it}^2 / g$  (Durán et al., 2011; Martin & Kok, 2017). However, saltation on Titan is characterized by much longer hop times than on Earth due to the higher air density, thus higher air drag, and smaller gravity. It follows that particle speeds in the upper part of the saltation layer can scale with  $u_*$  without producing a strong increase in impact velocity. Assuming similar proportions in the populations of grains in saltation and in reptation near the surface (Andreotti, 2004; Lämmel et al., 2012), the mean hop length on Titan scales as  $L \sim u_{*,it} (u_* + u_{*,it}) / g$ . The proposed scalings for  $L$  and  $\langle \Delta v \rangle$  on Titan are confirmed by COMSALT simulations (see Section S7 in Supporting Information S1) and yield a mass flux

$$Q = A \frac{\rho_f}{g} (u_*^2 - u_{*,it}^2) (u_* + u_{*,it}) \eta_q, \quad (6)$$

where  $A \approx 2.3$  is a dimensionless scaling coefficient and  $\eta_q \in (0, 1)$  is the intermittency factor that quantifies the fraction of time that saltation is active when the unsteady wind speeds oscillate between the impact and fluid thresholds (Lorenz et al., 1995). We calculate  $\eta_q$  using the parameterization of Comola, Kok et al. (2019), which was validated using extensive field data from three different locations on Earth. This parameterization predicts transport intermittency based on the friction velocity and the Obukhov stability parameter, which quantifies the shear-generated and buoyancy-generated turbulence driving the variability in wind speed (Murdoch et al., 2017; Panofsky et al., 1977) (see Section S6 in Supporting Information S1 for details). We find that the mass fluxes predicted with Equation 6 are in good agreement with steady-state mass fluxes obtained with COMSALT for a variety of particle sizes and friction velocities (Figure 3a).

The mass flux scaling  $Q \propto u_*^3$  of Equation 6 is typical of particle flows that dissipate energy through a combination of fluid drag, particle-bed collisions, and binary collisions between airborne grains (Pächt & Durán, 2020) and is found in another mass flux parameterization by Kawamura (1951), which has been commonly used in planetary saltation studies (e.g., Charnay et al., 2015; Gebhardt et al., 2020; Lee & Thomas, 1995; White, 1979). However, in the original parameterization by Kawamura (1951) it is assumed that fluid lifting drives continuous sediment transport and that the friction velocity at the bed, for which the threshold friction velocity is a proxy in the mass flux equation, is equal to the fluid threshold. We find that our parameterization that accounts for transport intermittency (Equation 6) predicts a significantly larger mass flux than the continuous transport parameterization by Kawamura (1951) when the wind speed lies between the impact and fluid thresholds, as is often the case on Titan (Figure 3b).

## 6. Aeolian Activity on Titan

We assess the aeolian transport potential of Titan's prevailing circulation by implementing the proposed mass flux parameterization (Equation 6) in the TAM (Lora et al., 2015, 2019) accounting for the effect of large-scale topography (Corlies et al., 2017) (see Section S8 in Supporting Information S1 for additional detail). We perform runtime calculations of the wind-driven saltation mass flux for 30 Titan years, using surface friction velocities and intermittency factors computed at the model time step of 10 min.

The model results indicate that sediment transport on Titan occurs in highly intermittent conditions, with daily-averaged intermittency factors  $\eta_q$  rarely exceeding 10% (Figure 4a). Furthermore, the daily-average mass fluxes in

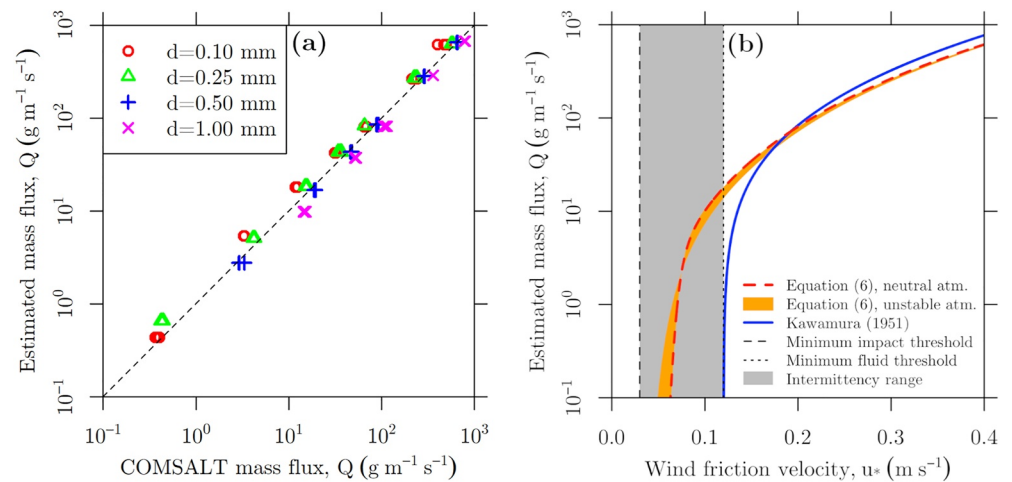


**Figure 3.** Saltation mass flux scaling for Titan conditions. (a) Comparison of mass fluxes predicted by comprehensive numerical model of steady state saltation and estimated with Equation 6 for different combinations of particle size and wind friction velocity. Because COMSALT simulates continuous transport, we assumed  $\eta_q = 1$  in Equation 6. (b) Titan mass flux scaling predicted with Equation 6 in conditions of intermittent transport for a neutrally stable atmosphere (dashed red line) and an unstable atmosphere (shaded orange area). To represent the unstable atmospheric conditions, we assigned an Obukhov length  $L_{MO} = -15$  m and a boundary layer depth spanning the range 300–3,000 m (Charnay & Lebonnois, 2012; Lorenz et al., 2010) (see supporting information for details on how these variables influence  $\eta_q$ ). The solid blue line represents the mass flux equation by Kawamura (1951) commonly used in planetary aeolian transport studies. We assumed that grain sizes on Titan lie within the range 0.05–2 mm, similar to sand on Earth, and set the impact and fluid thresholds equal to the corresponding minima in this range, that is  $u_{s, it} = 0.03$  m s<sup>-1</sup> (dashed black line) and  $u_{s, ft} = 0.12$  m s<sup>-1</sup> (dotted black line). The gray area indicates the range of saltation intermittency between the impact and fluid thresholds.

the equatorial region lie below 10 gm<sup>-1</sup> s<sup>-1</sup> (Figure 4b), which are typical of the intermittent transport regime (gray area in Figure 3b). Nevertheless, the cumulative mass fluxes in the equatorial region reach significant values at longer time scales (Figure 4c), with yearly mass fluxes of the order of 10<sup>4</sup> kg m<sup>-1</sup> (note that one Titan year corresponds to approximately 29.5 Earth years).

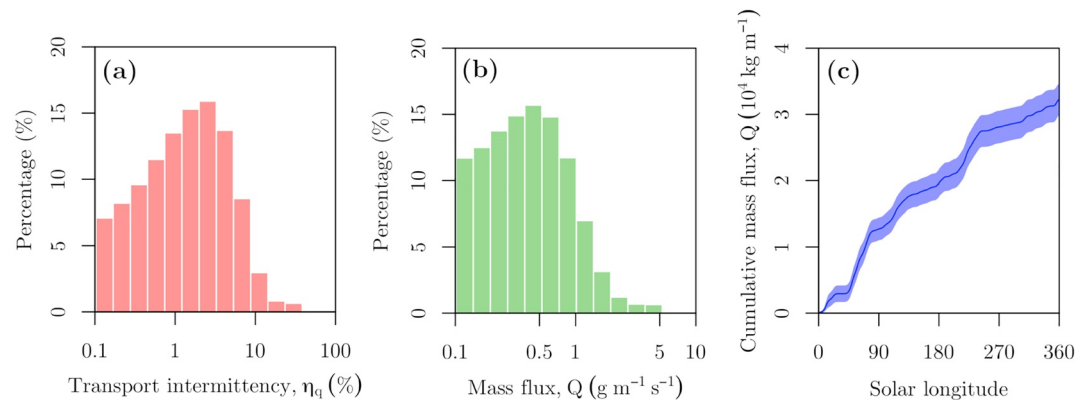


**Figure 4.** Sediment transport rates and intermittency on Titan. (a) Frequency distribution of daily-averaged intermittency factors  $\eta_q$  calculated in Titan Atmospheric Model (TAM) in the equatorial region of Titan (15°S–15°N, 384 grid points) for 30 years of simulation. (b) Frequency distribution of daily-averaged saltation mass fluxes calculated in TAM in the equatorial region of Titan for 30 years of simulation. (c) Cumulative mass fluxes predicted by TAM in the equatorial region. The solid line indicates the average of the 30 years and the shaded area indicates the spatial variability (standard error).

## 7. Discussion

We combined experimental results, theory, and modeling to investigate the conditions that lead to sediment transport initiation and cessation on Titan. For this purpose, we assumed that the cohesive forces measured for tholins at the microscale (Yu et al., 2017) apply to sand-sized grains on Titan. We found that cohesion significantly affects the wind speed required to lift grains from the surface, but not the wind speed required to sustain saltation through granular splash. We found that the minimum fluid threshold ( $u_* \approx 0.12 \text{ m s}^{-1}$ ) corresponds to a particle size  $d \approx 2 \text{ mm}$ , whereas the minimum impact threshold ( $u_* \approx 0.03 \text{ m s}^{-1}$ ) corresponds to a particle size  $d \approx 0.1 \text{ mm}$  (Figure 2). Furthermore, the impact threshold is smaller than the fluid threshold for grains smaller than 2 mm, whereas the fluid threshold is smaller than the impact threshold for larger grains. The granular splash process is thus more effective than aerodynamic forces in lifting submillimeter grains from the surface. Conversely, transport of supermillimeter grains is primarily sustained by aerodynamic entrainment, which typically occurs in dense fluid flows such as fluvial environments on Earth (Pächtz et al., 2020). It is noteworthy that the fluid threshold values predicted by Equation 1 are representative of wind tunnel conditions, where turbulence scales are much smaller than in the atmospheric boundary layer. Because the aerodynamic entrainment is predominantly caused by turbulent fluctuation events (Pächtz et al., 2020), it is possible that the fluid threshold on Titan may be up to 50% smaller than what is predicted by Equation 1 due to the large turbulent motions in the thick boundary layer (Pächtz et al., 2018). Despite these uncertainties, the separation between the minimum fluid and impact thresholds on Titan is likely to be significantly larger than on Earth (Ho et al., 2011; Martin & Kok, 2018). Much like saltation on Mars, Titan saltation may therefore be characterized by a process of hysteresis whereby the occurrence of transport below the fluid threshold depends on the history of the wind, that is, saltation occurs only if transport was initiated ( $u_* > u_{*,ft}$ ) more recently than it was terminated ( $u_* < u_{*,it}$ ) (e.g., Kok, 2010a).

We investigated the size of saltating grains on Titan by evaluating the ratio between settling velocity and friction velocity,  $w_s/u_*$ , for a wide range of grain sizes. We found that the size range of saltating grains may depend on the wind speed, varying from 0.2 to 2 mm near the fluid threshold to 0.05–0.1 mm near the impact threshold. If saltation on Titan were driven by aerodynamic entrainment, as traditionally assumed, Titan dunes would then be formed by coarse grains up to 2 mm in size. However, because general circulation models suggest that the friction velocity in Titan's equatorial region normally lies near the transport cessation threshold, we expect Titan dunes to be formed primarily by the finer grain fraction. Note that our analysis based on the equal susceptibility assumption may provide incorrect estimations of the size of saltating grains if some grain sizes are more susceptible to motion than others. For instance, Sullivan and Kok (2017) have found that 0.1 mm grains are prevalent in actively migrating ripples on Mars even though  $w_s/u_{*,ft}$  is much larger than one for this particle size.

Our analyses further indicated that the saltation mass flux on Titan scales with the third power of the wind friction velocity, that is,  $Q \propto u_*^3$  (Equation 6 and Figure 3). This suggests a higher sensitivity of the transport rate to the wind speed compared to Earth conditions, where  $Q \propto u_*^2$  (Martin & Kok, 2017). However, the larger separation between the fluid and impact thresholds on Titan, combined with the typically low wind speeds of the prevailing circulation, is more likely to cause intermittent transport than on Earth (Comola, Kok et al., 2019). We implemented the proposed mass flux scaling in the Titan general circulation model TAM and estimated that the prevailing circulation is capable of driving sediment transport rates of the order of  $10^4 \text{ kg m}^{-1}$  per Titan year (Figure 4a), which corresponds to a 10 m-high dune moving at approximately 1–5 m per Titan year. Titan's prevailing circulation may therefore play a fundamental role in driving the formation of the gigantic linear dunes revealed by the Cassini-Huygens mission (Radebaugh, 2013). Nonetheless, at that migration rate more than a century of observations would be needed to detect the migration of one of Titan's 100 m-high dunes with 100 m-resolution data from orbit (Ewing et al., 2015; Lorenz, 2014). Our TAM simulations indicate that transport intermittency causes saltation to be active approximately 1%–10% of the year (Figure 4b), with significant seasonal variations (Figure 4b). Overall, our analyses indicated that Titan's weak prevailing winds are capable of generating a significant “background” aeolian activity with critical implications for Titan's geomorphology and landscape evolution.

## Data Availability Statement

All data presented in this paper are available for download at the following repository <https://data.mendeley.com/datasets/97j874sph6/1>.

### Acknowledgments

This research was supported by the Swiss National Science Foundation (project number P2ELP2\_178219). X. Yu is supported by the 51 Pegasi b postdoctoral fellowship from the Heising-Simons Foundation. Additional support was provided by NASA Outer Planets Research grant NNX14AR23G to J. F. Kok. The authors thank Tetsuya Tokano, Claire Newman, Kirby Runyon, and Benjamin Charnay for sharing their Titan general and regional circulation model outputs. The authors also wish to thank Thomas Pähtz for the insightful discussions on the uncertainty in the fluid threshold value and the effect of the viscous sublayer on the impact threshold.

### References

- Ammi, M., Oger, L., Beladjine, D., & Valance, A. (2009). Three-dimensional analysis of the collision process of a bead on a granular packing. *Physical Review - Statistical Physics, Plasmas, Fluids, and Related Interdisciplinary Topics*, 79(2), 021305. <https://doi.org/10.1103/PhysRevE.79.021305>
- Anderson, R. S., & Haff, P. K. (1991). Wind modification and bed response during saltation of sand in air. In *Aeolian grain transport* (Vol. 1, pp. 21–51). Springer.
- Andreotti, B. (2004). A two-species model of aeolian sand transport. *Journal of Fluid Mechanics*, 510, 47–70. <https://doi.org/10.1017/S0022112004009073>
- Bagnold, R. A. (1937). The transport of sand by wind. *Geographical Journal*, 89(5), 409–438.
- Burr, D. M., Bridges, N. T., Marshall, J. R., Smith, J. K., White, B. R., & Emery, J. P. (2015). Higher-than-predicted saltation threshold wind speeds on Titan. *Nature*, 517(7532), 60–63. <https://doi.org/10.1038/nature14088>
- Charnay, B., Barth, E., Rafkin, S., Nartean, C., Lebonnois, S., Rodriguez, S., et al. (2015). Methane storms as a driver of Titan's dune orientation. *Nature Geoscience*, 8(5), 362–366. <https://doi.org/10.1038/ngeo2406>
- Charnay, B., & Lebonnois, S. (2012). Two boundary layers in Titan's lower troposphere inferred from a climate model. *Nature Geoscience*, 5(2), 106–109. <https://doi.org/10.1038/ngeo1374>
- Chepil, W. S. (1945). Dynamics of wind erosion: II. Initiation of soil movement. *Soil Science*, 60(5), 397.
- Comola, F., Gaume, J., Kok, J. F., & Lehning, M. (2019). Cohesion-induced enhancement of aeolian saltation. *Geophysical Research Letters*, 46, 5566–5574. <https://doi.org/10.1029/2019GL082195>
- Comola, F., Kok, J. F., Chamecki, M., & Martin, R. L. (2019). The intermittency of wind-driven sand transport. *Geophysical Research Letters*, 46, 13430–13440. <https://doi.org/10.1029/2019GL085739>
- Comola, F., & Lehning, M. (2017). Energy- and momentum-conserving model of splash entrainment in sand and snow saltation. *Geophysical Research Letters*, 44, 1601–1609. <https://doi.org/10.1002/2016GL071822>
- Corlies, P., Hayes, A. G., Birch, S. P. D., Lorenz, R., Stiles, B. W., Kirk, R., et al. (2017). Titan's topography and shape at the end of the Cassini mission. *Geophysical Research Letters*, 44, 11754–11761. <https://doi.org/10.1002/2017GL075518>
- Corn, M. (1961). The adhesion of solid particles to solid surfaces, I. A review. *Journal of the Air Pollution Control Association*, 11(11), 523–528. <https://doi.org/10.1080/00022470.1961.10468032>
- Durán, O., Claudin, P., & Andreotti, B. (2011). On aeolian transport: Grain-scale interactions, dynamical mechanisms and scaling laws. *Aeolian Research*, 3(3), 243–270. <https://doi.org/10.1016/j.aeolia.2011.07.006>
- Ewing, R. C., Hayes, A. G., & Lucas, A. (2015). Sand dune patterns on Titan controlled by long-term climate cycles. *Nature Geoscience*, 8(1), 15–19. <https://doi.org/10.1038/ngeo2323>
- Faulk, S. P., Lora, J. M., Mitchell, J. L., & Milly, P. C. D. (2020). Titan's climate patterns and surface methane distribution due to the coupling of land hydrology and atmosphere. *Nature Astronomy*, 4(4), 390–398. <https://doi.org/10.1038/s41550-019-0963-0>
- Fletcher, B. (1976). The incipient motion of granular materials. *Journal of Physics D: Applied Physics*, 9(17), 2471. <https://doi.org/10.1088/0022-3727/9/17/007>
- Gebhardt, C., Abuelgasim, A., Fonseca, R. M., Martín-Torres, J., & Zorzano, M.-P. (2020). Fully interactive and refined resolution simulations of the Martian dust cycle by the MarsWRF model. *Journal of Geophysical Research: Planets*, 125, e2019JE006253. <https://doi.org/10.1029/2019JE006253>
- Greeley, R., & Iversen, J. D. (1985). *Wind as a geological process: On Earth, Mars, Venus and Titan*. Cambridge University Press.
- He, C., Hörst, S. M., Riemer, S., Sebree, J. A., Pauley, N., & Vuitton, V. (2017). Carbon monoxide affecting planetary atmospheric chemistry. *The Astrophysical Journal Letters*, 841(2), L31.
- Ho, T. D., Valance, A., Dupont, P., & Ould El Moctar, A. (2011). Scaling laws in Aeolian sand transport. *Physical Review Letters*, 106(9), 094501. <https://doi.org/10.3847/2041-8213/aa74cc>
- Hörst, S. M., & Tolbert, M. A. (2013). In situ measurements of the size and density of Titan aerosol analogs. *The Astrophysical Journal Letters*, 770(1), L10. <https://doi.org/10.1088/2041-8205/770/1/L10>
- Imanaka, H., Cruikshank, D. P., Khare, B. N., & McKay, C. P. (2012). Optical constants of Titan tholins at mid-infrared wavelengths (2.5–25  $\mu\text{m}$ ) and the possible chemical nature of Titan's haze particles. *Icarus*, 218(1), 247–261. <https://doi.org/10.1016/j.icarus.2011.11.018>
- Israelachvili, J. N. (1986). *Intermolecular and surface forces*. Wiley Online Library.
- Iversen, J. D., Pollack, J. B., Greeley, R., & White, B. R. (1976). Saltation threshold on Mars: The effect of interparticle force, surface roughness, and low atmospheric density. *Icarus*, 29(3), 381–393. [https://doi.org/10.1016/0019-1035\(76\)90140-8](https://doi.org/10.1016/0019-1035(76)90140-8)
- Kawamura, R. (1951). Study on sand movement by wind. *Annual Report Institute Science and Technology*, 5(95–112), 95–112.
- Kok, J. F. (2010a). Difference in the wind speeds required for initiation versus continuation of sand transport on Mars: Implications for dunes and dust storms. *Physical Review Letters*, 104(7), 074502. <https://doi.org/10.1103/PhysRevLett.104.074502>
- Kok, J. F. (2010b). An improved parameterization of wind-blown sand flux on Mars that includes the effect of hysteresis. *Geophysical Research Letters*, 37. <https://doi.org/10.1029/2010GL043646>
- Kok, J. F., Parteli, E. J. R., Michaels, T. I., & Karam, D. B. (2012). The physics of wind-blown sand and dust. *Reports on Progress in Physics*, 75(10), 106901. <https://doi.org/10.1088/0034-4885/75/10/106901>
- Kok, J. F., & Renno, N. O. (2009). A comprehensive numerical model of steady state saltation (COMSALT). *Journal of Geophysical Research*, 114, D17204. <https://doi.org/10.1029/2009JD011702>
- Lämmel, M., Rings, D., & Kroy, K. (2012). A two-species continuum model for aeolian sand transport. *New Journal of Physics*, 14(9), 093037. <https://doi.org/10.1088/1367-2630/14/9/093037>
- Lebonnois, S., Burgalat, J., Rannou, P., & Charnay, B. (2012). Titan global climate model: A new 3-dimensional version of the IPSL Titan GCM. *Icarus*, 218(1), 707–722. <https://doi.org/10.1016/j.icarus.2011.11.032>
- Lee, P., & Thomas, P. C. (1995). Longitudinal dunes on Mars: Relation to current wind regimes. *Journal of Geophysical Research*, 100(E3), 5381–5395. <https://doi.org/10.1029/95JE00225>
- Lopes, R. M. C., Wall, S. D., Elachi, C., Birch, S. P. D., Corlies, P., Coustenis, A., et al. (2019). Titan as revealed by the Cassini radar. *Space Science Reviews*, 215(4), 1–50. <https://doi.org/10.1007/s11214-019-0598-6>
- Lora, J. M., Lunine, J. I., & Russell, J. L. (2015). GCM simulations of Titan's middle and lower atmosphere and comparison to observations. *Icarus*, 250, 516–528. <https://doi.org/10.1016/j.icarus.2014.12.030>
- Lora, J. M., Tokano, T., d'Ollone, J. V., Lebonnois, S., & Lorenz, R. D. (2019). A model intercomparison of Titan's climate and low-latitude environment. *Icarus*, 333, 113–126. <https://doi.org/10.1016/j.icarus.2019.05.031>

- Lorenz, R. D. (2014). Physics of saltation and sand transport on Titan: A brief review. *Icarus*, 230, 162–167. <https://doi.org/10.1016/j.icarus.2013.06.023>
- Lorenz, R. D., Claudin, P., Andreotti, B., Radebaugh, J., & Tokano, T. (2010). A 3 km atmospheric boundary layer on Titan indicated by dune spacing and Huygens data. *Icarus*, 205(2), 719–721. <https://doi.org/10.1016/j.icarus.2009.08.002>
- Lorenz, R. D., Lunine, J. I., Grier, J. A., & Fisher, M. A. (1995). Prediction of aeolian features on planets: Application to Titan paleoclimatology. *Journal of Geophysical Research*, 100(E12), 26377–26386. <https://doi.org/10.1029/95JE02708>
- Lorenz, R. D., Wall, S., Radebaugh, J., Boubin, G., Reffet, E., Janssen, M., et al. (2006). The sand seas of Titan: Cassini RADAR observations of longitudinal dunes. *Science*, 312(5774), 724–727. <https://doi.org/10.1126/science.1123257>
- Lorenz, R. D., & Zimbelman, J. R. (2014). *Dune worlds: How windblown sand shapes planetary landscapes*. Springer Science & Business Media.
- MacKenzie, S. M., Birch, S. P. D., Hörst, S. M., Sotin, C., Barth, E., Lora, J. M., et al. (2021). Titan: Earth-like on the outside, ocean world on the inside. *The Planetary Science Journal*, 2(3), 112. arXiv preprint arXiv:2102.08472. <https://doi.org/10.48550/arXiv.2102.08472>
- Martin, R. L., & Kok, J. F. (2017). Wind-invariant saltation heights imply linear scaling of aeolian saltation flux with shear stress. *Science Advances*, 3(6), e1602569. <https://doi.org/10.1126/sciadv.1602569>
- Martin, R. L., & Kok, J. F. (2018). Distinct thresholds for the initiation and cessation of aeolian saltation from field measurements. *Journal of Geophysical Research: Earth*, 123, 1546–1565. <https://doi.org/10.1029/2017JF004416>
- Martin, R. L., & Kok, J. F. (2019). Size-independent susceptibility to transport in aeolian saltation. *Journal of Geophysical Research: Earth Surface*, 124, 1658–1674. <https://doi.org/10.1029/2019JF005104>
- McCord, T. B., Hansen, G. B., Buratti, B. J., Clark, R. N., Cruikshank, D. P., D'Aversa, E., et al. (2006). Composition of Titan's surface from Cassini VIMS. *Planetary and Space Science*, 54(15), 1524–1539. <https://doi.org/10.1016/j.pss.2006.06.007>
- Méndez-Harper, J. S., McDonald, G. D., Dufek, J., Malaska, M. J., Burr, D. M., Hayes, A. G., et al. (2017). Electrification of sand on Titan and its influence on sediment transport. *Nature Geoscience*, 10(4), 260–265. <https://doi.org/10.1038/ngeo2921>
- Murdoch, N., Mimoun, D., Garcia, R. F., Rapin, W., Kawamura, T., Lognonné, P., et al. (2017). Evaluating the wind-induced mechanical noise on the InSight seismometers. *Space Science Reviews*, 211(1), 429–455. <https://doi.org/10.1007/s11214-016-0311-y>
- Nalpanis, P., Hunt, J. C. R., & Barrett, C. F. (1993). Saltating particles over flat beds. *Journal of Fluid Mechanics*, 251, 661–685. <https://doi.org/10.1017/S0022112093003568>
- Newman, C. E., Richardson, M. I., Lian, Y., & Lee, C. (2016). Simulating Titan's methane cycle with the TitanWRF general circulation model. *Icarus*, 267, 106–134. <https://doi.org/10.1016/j.icarus.2015.11.028>
- Nishimura, K., & Hunt, J. C. R. (2000). Saltation and incipient suspension above a flat particle bed below a turbulent boundary layer. *Journal of Fluid Mechanics*, 417, 77–102. <https://doi.org/10.1017/S0022112000001014>
- Pächt, T., Clark, A. H., Valyrakis, M., & Durán, O. (2020). The physics of sediment transport initiation, cessation, and entrainment across aeolian and fluvial environments. *Review of Geophysics*, 58(1), e2019RG000679. <https://doi.org/10.1029/2019RG000679>
- Pächt, T., & Durán, O. (2018). The cessation threshold of nonsuspended sediment transport across aeolian and fluvial environments. *Journal of Geophysical Research: Earth Surface*, 123, 1638–1666. <https://doi.org/10.1029/2017JF004580>
- Pächt, T., & Durán, O. (2020). Unification of aeolian and fluvial sediment transport rate from granular physics. *Physical Review Letters*, 124(16), 168001. <https://doi.org/10.1103/PhysRevLett.124.168001>
- Pächt, T., Liu, Y., Xia, Y., Hu, P., He, Z., & Tholen, K. (2021). Unified model of sediment transport threshold and rate across weak and intense subaqueous bedload, windblown sand, and windblown snow. *Journal of Geophysical Research: Earth Surface*, 126, e2020JF005859. <https://doi.org/10.1029/2020JF005859>
- Pächt, T., Valyrakis, M., Zhao, X., & Li, Z. (2018). The critical role of the boundary layer thickness for the initiation of aeolian sediment transport. *Geosciences*, 8(9), 314. <https://doi.org/10.3390/geosciences8090314>
- Panofsky, H. A., Tennekes, H., Lenschow, D. H., & Wyngaard, J. C. (1977). The characteristics of turbulent velocity components in the surface layer under convective conditions. *Boundary-Layer Meteorology*, 11(3), 355–361. <https://doi.org/10.1007/BF02186086>
- Radebaugh, J. (2013). Dunes on Saturn's moon Titan as revealed by the Cassini mission. *Aeolian Research*, 11, 23–41. <https://doi.org/10.1016/j.aeolia.2013.07.001>
- Radebaugh, J., Lorenz, R., Farr, T., Paillou, P., Savage, C., & Spencer, C. (2010). Linear dunes on Titan and Earth: Initial remote sensing comparisons. *Geomorphology*, 121(1–2), 122–132. <https://doi.org/10.1016/j.geomorph.2009.02.022>
- Radebaugh, J., Lorenz, R. D., Lunine, J. I., Wall, S. D., Boubin, G., Reffet, E., et al. (2008). Dunes on Titan observed by Cassini RADAR. *Icarus*, 194(2), 690–703. <https://doi.org/10.1016/j.icarus.2007.10.015>
- Rice, M. A., Willetts, B. B., & McEwan, I. K. (1995). An experimental study of multiple grain-size ejecta produced by collisions of saltating grains with a flat bed. *Sedimentology*, 42(4), 695–706. <https://doi.org/10.1111/j.1365-3091.1995.tb00401.x>
- Rice, M. A., Willetts, B. B., & McEwan, I. K. (1996). Observations of collisions of saltating grains with a granular bed from high-speed cine-film. *Sedimentology*, 43(1), 21–31.
- Rodríguez, S., Le Mouélic, S., Barnes, J. W., Kok, J. F., Rafkin, S. C. R., Lorenz, R. D., et al. (2018). Observational evidence for active dust storms on Titan at equinox. *Nature Geoscience*, 11(10), 727–732. <https://doi.org/10.1038/s41561-018-0233-2>
- Shao, Y., & Lu, H. (2000). A simple expression for wind erosion threshold friction velocity. *Journal of Geophysical Research*, 105(D17), 22437–22443. <https://doi.org/10.1029/2000JD900304>
- Soderblom, L. A., Kirk, R. L., Lunine, J. I., Anderson, J. A., Baines, K. H., Barnes, J. W., et al. (2007). Correlations between Cassini VIMS spectra and RADAR SAR images: Implications for Titan's surface composition and the character of the Huygens Probe landing site. *Planetary and Space Science*, 55(13), 2025–2036. <https://doi.org/10.1016/j.pss.2007.04.014>
- Sullivan, R., & Kok, J. F. (2017). Aeolian saltation on Mars at low wind speeds. *Journal of Geophysical Research: Planets*, 122, 2111–2143. <https://doi.org/10.1002/2017JE005275>
- Tokano, T. (2010). Relevance of fast westerlies at equinox for the eastward elongation of Titan's dunes. *Aeolian Research*, 2(2–3), 113–127. <https://doi.org/10.1016/j.aeolia.2010.04.003>
- Ungar, J. E., & Haff, P. K. (1987). Steady state saltation in air. *Sedimentology*, 34(2), 289–299. <https://doi.org/10.1111/j.1365-3091.1987.tb00778.x>
- White, B. R. (1979). Soil transport by winds on Mars. *Journal of Geophysical Research*, 84(B9), 4643–4651. <https://doi.org/10.1029/JB084iB09p04643>
- Willetts, B. B., & Rice, M. A. (1986). Collisions in aeolian saltation. *Acta Mechanica*, 63(1–4), 255–265. <https://doi.org/10.1007/BF01182552>
- Willetts, B. B., & Rice, M. A. (1989). Collisions of quartz grains with a sand bed: The influence of incident angle. *Earth Surface Processes and Landforms*, 14(8), 719–730. <https://doi.org/10.1002/esp.3290140806>
- Yu, X., Hörst, S. M., He, C., & McGuiggan, P. (2020). Single particle triboelectrification of Titan sand analogs. *Earth and Planetary Science Letters*, 530, 115996. <https://doi.org/10.1016/j.epsl.2019.115996>

- Yu, X., Hörst, S. M., He, C., McGuiggan, P., & Bridges, N. T. (2017). Direct measurement of interparticle forces of Titan aerosol analogs ("tholin") using atomic force microscopy. *Journal of Geophysical Research*, *122*(12), 2610–2622. <https://doi.org/10.1002/2017je005437>
- Yu, X., Hörst, S. M., He, C., McGuiggan, P., Kristiansen, K., & Zhang, X. (2020). Surface energy of the Titan aerosol analog "tholin". *The Astrophysical Journal*, *905*(2), 88.
- Zingg, A. W. (1953). Wind tunnel studies of the movement of sedimentary material. In *Proc. 5th Hydraulics Conference Bulletin* (pp. 111–135). Inst. of Hydraulics Iowa City.

## References From the Supporting Information

- Akyildiz, F., Jones, R. S., & Walters, K. (1990). On the spring-dashpot representation of linear viscoelastic behaviour. *Rheologica Acta*, *29*(5), 482–484. <https://doi.org/10.1007/bf01376800>
- Anderson, R. S., & Haff, P. K. (1988). Simulation of eolian saltation. *Science*, *241*(4867), 820–823. <https://doi.org/10.1126/science.241.4867.820>
- Bagnold, R. A. (1941). *The physics of blown sand and desert dunes*.
- Barndorff-Nielsen, O. E. (1986). Sand, wind and statistics: Some recent investigations. *Acta Mechanica*, *64*(1–2), 1–18. <https://doi.org/10.1007/bf01180094>
- Battalio, J. M., & Lora, J. M. (2021). Global impacts from high-latitude storms on Titan. *Geophysical Research Letters*, *48*(18), e2021GL094244. <https://doi.org/10.1029/2021gl094244>
- Beladjine, D., Ammi, M., Oger, L., & Valance, A. (2007). Collision process between an incident bead and a three-dimensional granular packing. *Physical Review E - Statistical Physics, Plasmas, Fluids, and Related Interdisciplinary Topics*, *75*(6), 061305. <https://doi.org/10.1103/physreve.75.061305>
- Carneiro, M. V., Araújo, N. A. M., Pähtz, T., & Herrmann, H. J. (2013). Midair collisions enhance saltation. *Physical Review Letters*, *111*(5), 058001. <https://doi.org/10.1103/physrevlett.111.058001>
- Chu, C. R., Parlange, M. B., Katul, G. G., & Albertson, J. D. (1996). Probability density functions of turbulent velocity and temperature in the atmospheric surface layer. *Water Resources Research*, *32*(6), 1681–1688. <https://doi.org/10.1029/96wr00287>
- Colbeck, S. C. (1986). Statistics of coarsening in water-saturated snow. *Acta Metallurgica et Materialia*, *34*(3), 347–352. [https://doi.org/10.1016/0001-6160\(86\)90070-2](https://doi.org/10.1016/0001-6160(86)90070-2)
- Crassous, J., Beladjine, D., & Valance, A. (2007). Impact of a projectile on a granular medium described by a collision model. *Physical Review Letters*, *99*(24), 248001. <https://doi.org/10.1103/physrevlett.99.248001>
- Cundall, P. A., & Strack, O. D. L. (1979). A discrete numerical model for granular assemblies. *Géotechnique*, *29*(1), 47–65. <https://doi.org/10.1680/geot.1979.29.1.47>
- German, R. M. (2014). Coordination number changes during powder densification. *Powder Technology*, *253*, 368–376. <https://doi.org/10.1016/j.powtec.2013.12.006>
- Gold, L. W. (1958). Some observations on the dependence of strain on stress for ice. *Canadian Journal of Physics*, *36*(10), 1265–1275. <https://doi.org/10.1139/p58-131>
- Gordon, M., & McKenna-Neuman, C. (2011). A study of particle splash on developing ripple forms for two bed materials. *Geomorphology*, *129*(1–2), 79–91. <https://doi.org/10.1016/j.geomorph.2011.01.015>
- Haff, P. K., & Anderson, R. S. (1993). Grain scale simulations of loose sedimentary beds: The example of grain-bed impacts in aeolian saltation. *Sedimentology*, *40*(2), 175–198. <https://doi.org/10.1111/j.1365-3091.1993.tb01760.x>
- Itasca Consulting Group. (2014). *PFC - Particle Flow Code* (Vol. 50).
- Iversen, J. D., & Rasmussen, K. R. (1994). The effect of surface slope on saltation threshold. *Sedimentology*, *41*(4), 721–728. <https://doi.org/10.1111/j.1365-3091.1994.tb01419.x>
- Kolmogorov, A. N. (1941). On the logarithmic normal distribution of particle sizes under grinding. *Proceedings of the USSR Academy of Science*, *31*, 99–101.
- Li, B., & McKenna Neuman, C. (2012). Boundary-layer turbulence characteristics during aeolian saltation. *Geophysical Research Letters*, *39*(11). <https://doi.org/10.1029/2012gl052234>
- Lora, J. M., & Ádámkóvics, M. (2017). The near-surface methane humidity on Titan. *Icarus*, *286*, 270–279. <https://doi.org/10.1016/j.icarus.2016.10.012>
- Lorenz, R. D. (2021). An engineering model of Titan surface winds for Dragonfly landed operations. *Advances in Space Research*, *67*(7), 2219–2230. <https://doi.org/10.1016/j.asr.2021.01.023>
- Mellor, G. L., & Yamada, T. (1982). Development of a turbulence closure model for geophysical fluid problems. *Review of Geophysics*, *20*(4), 851–875. <https://doi.org/10.1029/rg020i004p00851>
- Mitha, S., Tran, M. Q., Werner, B. T., & Haff, P. K. (1986). The grain-bed impact process in aeolian saltation. *Acta Mechanica*, *63*(1–4), 267–278. <https://doi.org/10.1007/bf01182553>
- Nikuradse, J. (1933). Strömungsgesetze in rauhen Röhren. *VDI-Forschungsheft*, *361*, 1.
- Pähtz, T., Kok, J. F., & Herrmann, H. J. (2012). The apparent roughness of a sand surface blown by wind from an analytical model of saltation. *New Journal of Physics*, *14*(4), 043035. <https://doi.org/10.1088/1367-2630/14/4/043035>
- Potyondy, D. O., & Cundall, P. A. (2004). A bonded-particle model for rock. *International Journal of Rock Mechanics and Mining Sciences*, *41*(8), 1329–1364. <https://doi.org/10.1016/j.ijrmms.2004.09.011>
- Rioual, F., Valance, A., & Bideau, D. (2000). Experimental study of the collision process of a grain on a two-dimensional granular bed. *Physical Review E - Statistical Physics, Plasmas, Fluids, and Related Interdisciplinary Topics*, *62*(2), 2450. <https://doi.org/10.1103/physreve.62.2450>
- Schmidt, R. A. (1980). Threshold wind-speeds and elastic impact in snow transport. *Journal of Glaciology*, *26*, 453–467. <https://doi.org/10.3189/s0022143000010972>
- Verlet, L. (1967). Computer "experiments" on classical fluids. I. thermodynamical properties of Lennard-Jones molecules. *Physics Reviews*, *159*(1), 98–193. <https://doi.org/10.1103/physrev.159.98>
- Willets, B. B., & Rice, M. A. (1985). Inter-saltation collisions. *Proc. Int. Workshop on physics of blown sand* (Vol. 1, pp. 83–100).
- Xing, M., & He, C. (2013). 3D ejection behavior of different sized particles in the grain-bed collision process. *Geomorphology*, *187*, 94–100. <https://doi.org/10.1016/j.geomorph.2013.01.002>